

Adversarial Sparse Teacher: Defense Against Distillation-Based Model Stealing Attacks Using Adversarial Examples

Eda Yilmaz

Hacettepe University
Computer Engineering Department
yilmaz-eda@hacettepe.edu.tr

Hacer Yalim Keles

Hacettepe University
Computer Engineering Department
hacerkeles@cs.hacettepe.edu.tr

Abstract

Knowledge Distillation (KD) facilitates the transfer of discriminative capabilities from an advanced teacher model to a simpler student model, ensuring performance enhancement without compromising accuracy. It is also exploited for model stealing attacks, where adversaries use KD to mimic the functionality of a teacher model. Recent developments in this domain have been influenced by the *Stingy Teacher* model, which provided empirical analysis showing that sparse outputs can significantly degrade the performance of student models. Addressing the risk of intellectual property leakage, our work introduces an approach to train a teacher model that inherently protects its logits, influenced by the *Nasty Teacher* concept. Differing from existing methods, we incorporate sparse outputs of adversarial examples with standard training data to strengthen the teacher’s defense against student distillation. Our approach carefully reduces the relative entropy between the original and adversarially perturbed outputs, allowing the model to produce adversarial logits with minimal impact on overall performance. The source codes will be made publicly available soon.

Keywords — Knowledge distillation, Adversarial examples, Model stealing defense

1 Introduction

In deep learning, the efficiency and performance of neural networks are highly important, particularly in applications where computational resources are limited. Knowledge Distillation (KD) introduces a method in this context, enabling the knowledge transfer from a complex, high-performing teacher model to a more simpler, efficient student model [1]. The realm of research surrounding this concept has significantly expanded. The methodology of KD can be broadly categorized based on the type of the knowledge transferred: output responses [1, 2], features [3–5], and relations [6–8]. Each category targets a different aspect of the teacher model’s intelligence; from its output predictions to the intermediate representations and the inter-layer interactions or relationship between samples, respectively [9]. An interesting technique of KD is Self Distillation, where a model is trained to distill knowledge from itself, effectively refining its performance without the need for an external teacher model [10, 11].

Knowledge distillation facilitates the deployment of powerful neural networks on resource limited devices and enhances the performance of smaller models. However, these methods has increased concerns regarding security of proprietary models through model stealing attacks. Such attacks aim to replicate the functionality of proprietary models without authorized access, posing significant threats to intellectual property and model integrity [12]. Various methods have been proposed to affirm ownership of machine learning models, including watermarking [13, 14] and passport-based protections [15, 16]. However, these methods remained insufficient in preventing the extraction of models.

The potential theft of valuable models necessitates proactive measures for prevention. A study called *Nasty Teacher* addresses this issue [17]. This method involves creating a secondary model,

derived from the base model, which is resistant to model stealing while maintaining comparable performance. The approach involves subtly altering the output logits of the secondary model, which effectively misleads any adversarial *student* models attempting to replicate it, without altering the primary behavior or performance of the model under standard conditions. To achieve this, the algorithm increases the relative entropy between the output distributions of the base and secondary models, utilizing Kullback-Leibler (KL) divergence [18], while simultaneously preserving high accuracy through minimization of cross-entropy loss.

An extension of this research, known as the *Stingy Teacher*, takes a different approach by directly inducing sparsity in the output logits. This method structures sparse logits by zeroing out class probabilities except for the top n classes prior to knowledge distillation, revealing only this reduced information [19]. This approach, theoretically validated to fail student models, inspired our method’s incorporation of sparsity. Like *Nasty Teacher*, our method aligns with the principle of maintaining a cautious teacher, but instead of applying modifications to the outputs, we integrate sparsity into the solution. This not only enhances the undistillability of the teacher but also addresses the challenges associated with creating a teacher model whose sparse outputs remain immutable in the face of distillation attempts.

Inspired by these studies, our work represents a novel defensive method called *Adversarial Sparse Teacher (AST)*. In contrast to the *Nasty Teacher* model, which advances learning by concurrently maximizing Kullback-Leibler (KL) divergence and minimizing cross-entropy loss, our approach adopts a contrary strategy. We prioritize *minimizing* all the terms in the loss, aiming to steer learning in a specific, well-defined direction. This approach ensures a more balanced path in optimization. Moreover, we propose and use a new divergence function, *Exponential Predictive Divergence (EPD)* that eliminates the unfavorable effects of KL Divergence during optimization. Our method employs *adversarial counterparts of the original images* to systematically generate ambiguous outputs relative to the given inputs. The non-random nature of these adversarial images ensures a consistent redundancy in the output logits, effectively deceiving potential model stealers.

The creation of adversarial examples is crucial for understanding their nature and impact on neural networks. Projected Gradient Descent (PGD) method, begins at a random point and iteratively applies perturbations until reaching the maximum allowed magnitude [20]. Furthermore, to enhance defense against adversarial attacks, defense strategies often incorporate adversarial examples into model training. This can involve training models directly on these examples or pairing the outputs from adversarial examples with those from clean examples. The Adversarial Logit Pairing (ALP) method [21] exemplifies this strategy by showing that minimizing the L2 distance between the logits of clean images and their adversarial counterparts mitigates adversarial attacks. This indicates that the features of adversarial images can be learned and countered through the analysis of logits.

Building upon these insights, our proposed teacher model includes a sparsity constraint, aiming to encapsulate adversarial information that maximizes ambiguity within its logits while preserving high accuracy. To achieve this, we defined a new loss function that distills from a sparse representation of the model’s response to adversarial images. To the best of our knowledge, this approach is novel in this domain. Our work makes two significant contributions to the field, summarized as follows:

- We introduce *Adversarial Sparse Teacher (AST)*, a novel methodology that leverages adversarial examples, sparse logits, and a unique loss function during training. This approach is designed to enhance the robustness of models against stealing attacks, addressing a critical concern in contemporary model security.
- We propose a new *divergence function (EPD)*, which provides an innovative method for assessing discrepancies between predicted and actual probability distributions. This function is particularly effective in highlighting significant variances in instances where predictions are made with high confidence. It thereby offers a more refined and sensitive tool for model evaluation and optimization. This contribution presents fresh insights and practical tools for researchers and practitioners, broadening the scope of methodologies available for model assessment and improvement.

2 Methodology

2.1 Knowledge Distillation

In the context of knowledge distillation, the objective is to train a student neural network, which is denoted as $f_{\theta_S}(\cdot)$, to mimic the behavior of a pre-trained teacher network, denoted as $f_{\theta_T}(\cdot)$. Both networks have their respective parameter sets: θ_T for the teacher network and θ_S for the student network. The training dataset is represented by \mathcal{X} , containing pairs of samples and their corresponding labels, denoted as $(x^{(i)}, y^{(i)})$. The logit response of a sample $x^{(i)}$ from the network $f_{\theta}(\cdot)$ is indicated by $p_{f_{\theta}}(x^{(i)})$. The *softmax temperature* function, $\sigma_{\tau_s}(\cdot)$, which is proposed by Hinton et al. in 2015, transforms logits into soft probabilities when a large temperature τ_s , which is usually greater than 1, is applied; and it behaves like the standard softmax function $\sigma(\cdot)$, when τ_s is set to 1 [1]. To achieve knowledge distillation, a combined loss function is utilized for training the student network, as shown in Eqn. (1).

$$\begin{aligned} \mathcal{L}_{KD} = \alpha \tau_S^2 \mathcal{L}_{KL}(\sigma_{\tau_s}(p_{f_{\theta_T}}(x^{(i)})), \sigma_{\tau_s}(p_{f_{\theta_S}}(x^{(i)}))) \\ + (1 - \alpha) \mathcal{L}_{CE}(\sigma(p_{f_{\theta_S}}(x^{(i)})), y^{(i)}) \end{aligned} \quad (1)$$

This combined loss function consists of two terms. The first term measures the KL divergence between the softened logits of the teacher network, $\sigma_{\tau_s}(p_{f_{\theta_T}}(x^{(i)}))$, and the student network, $\sigma_{\tau_s}(p_{f_{\theta_S}}(x^{(i)}))$. This divergence quantifies the difference in the distributions of soft probabilities generated by the two networks. The second term is the cross-entropy loss between the softened probabilities of the student network, $\sigma(p_{f_{\theta_S}}(x^{(i)}))$, and the ground truth label, $y^{(i)}$. This term ensures that the student network is learning to predict the correct labels directly.

To control the balance between knowledge distillation and conventional cost minimization, a hyperparameter α is usually used. By adjusting the value of α , the relative importance of knowledge transfer from the teacher network and the direct supervision of the student network can be controlled during the training process [1].

2.2 Producing Adversarial Examples

Projected Gradient Descent (PGD) is an iterative method used to generate adversarial examples. This process begins at a randomly selected location (within the ϵ -ball), starting from an original input x , and perturbs the image in the direction of maximum loss (Eqn. (2)). The magnitude of these perturbations is governed by a predefined step size, denoted as α , and the process is repeated for a specified number of steps. At each iteration, PGD ensures that the perturbations do not exceed the predefined size, ϵ , by projecting the perturbed input back into the valid space defined by the ϵ -ball [20]. Additionally, Mandry et al. [20] propose that training classifiers with adversarial examples crafted by PGD can enhance their robustness against various types of first-order attacks.

$$x^{(t+1)} = \text{Project}_{\epsilon} \left(x^{(t)} + \alpha \cdot \text{sign}(\nabla_x \mathcal{L}(\theta, x, y)) \right) \quad (2)$$

Adversarial examples are known for their property of transferability, wherein an example crafted for a specific network often tends to be misclassified by another network [22]. This indicates that a model is likely to transfer adversarial characteristics effectively across different network architectures. We strategically leverage this transferability characteristic in our approach to diminish the student model’s ability to accurately interpret and replicate information derived from the teacher model.

2.3 Sparse Logits

The *Stingy Teacher* work suggests that smoothness in the output distribution yields enhancements in the student model’s KD performance; the feature that renders a teacher model resistant to distillation

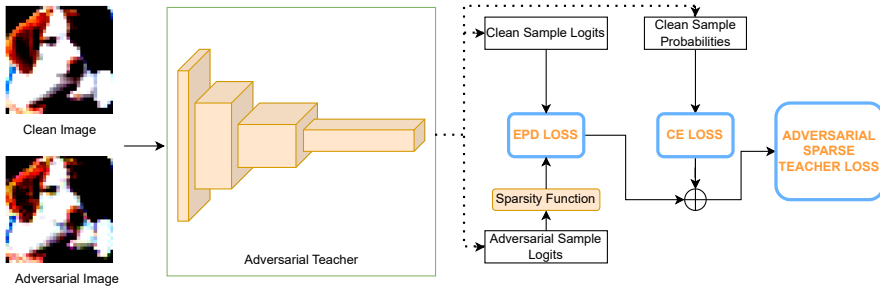


Fig. 1: Training scheme of *AST*. KL loss indicates Kullback-Liebler divergence loss and it uses logits of adversarial and clean samples. CE loss denotes Cross-entropy loss of clean sample probabilities and labels as usual. *AST* loss is sum of these two loss terms.

is the presence of sparsity in its outputs. This sparsity is achieved by retaining only the top n class probabilities in the logits, effectively focusing the model’s attention on the most significant classes while disregarding the less relevant ones. This methodology strategically channels the distillation process, degrades the performance of adversary [19].

2.4 Proposed Method: Adversarial Sparse Teacher

The primary objective of our study is to develop a teacher model that generates adversarial logits to disrupt the efficacy of models attempting to extract information from these outputs. This approach is only effective if the teacher model concurrently yields high accuracy for the correct categories. Therefore, the ultimate design goal is to mislead student models without compromising performance. To achieve this, we start by generating an adversarial version of the original dataset using a base model, which shares its architectural framework with the *Adversarial Sparse Teacher (AST)*. The data generated from these adversarial instances are then utilized in the training of our teacher model. Since adversarial examples are crafted to maximize the model’s loss, their outputs intrinsically embody this characteristic. In this context, we aim to reduce the relative entropy between the outputs of the *AST* for original and adversarial images, thus ensuring closer alignment (Fig. 1).

Concurrently, our method aims to reduce the model’s vulnerability by simultaneously diminishing the smoothness of the logits and augmenting data sparsity. Drawing from the foundational concepts of the *Stingy Teacher* approach, our strategy proposes a more robust and secure framework for model training. Unlike the *Stingy Teacher* method, which primarily relies on using the top n logits from the base model’s outputs to induce sparsity during the student model’s training—without the need for actively training a teacher model—our approach involves developing a teacher model that generates ambiguous outputs. This is achieved through an optimization process that promotes sparsity, utilizing adversarial examples. Importantly, this method retains much of the original accuracy of the base model. The key advantage of our approach is its practical application: by training a teacher model to inherently produce modified outputs, we effectively reduce the risk of the teacher model’s outputs being compromised or stolen. This not only preserves the integrity of the teacher model but also significantly bolsters its defense against extraction attacks, presenting a more secure and viable solution for real-world applications.

In this context, we defined the loss function of our model as in Eqn.(3).

$$\begin{aligned} \mathcal{L}_{AST} = \alpha\tau^2 \mathcal{L}_{EPD}(\sigma_\tau(p_{f_\theta}(x^{(i)})), \sigma_\tau(\text{sparse}(p_{f_\theta}(x_{adv}^{(i)}), \beta))) \\ + (1 - \alpha)\mathcal{L}_{CE}(\sigma(p_{f_\theta}(x^{(i)})), y^{(i)}) \end{aligned} \quad (3)$$

Here, the *AST* network is represented as $f_\theta(\cdot)$ with θ denoting the network’s parameters. Training dataset samples alongside their corresponding labels are denoted as $(x^{(i)}, y^{(i)})$, and samples’ adversarial counterparts are represented as $x_{adv}^{(i)}$. The logit response obtained from either $x^{(i)}$ or $x_{adv}^{(i)}$ by the network $f_\theta(\cdot)$ is denoted as $p_{f_\theta}(\cdot)$. The *sparse* function, accepts $p_{f_\theta}(\cdot)$ for a given sample and a

parameter β , which represents the sparsity ratio. This function is designed to return the sparse version of the logits. Additionally, the softmax temperature function is denoted as $\sigma_\tau(\cdot)$. An increase in the τ parameter, causes this function to yield a distribution characterized by higher entropy, more evenly spread probability across classes. The first term in the equation calculates our proposed *Exponential Predictive Divergence* between the logits of original images and sparse logits of the adversarial examples. Concurrently, the second term computes the cross-entropy loss of training samples and their labels. The goal of this proposed objective function is to minimize the sum of these two terms, thereby enhancing the model’s robustness and performance.

2.5 Exponential Predictive Divergence (EPD) Loss

In our research, we observed that using KL divergence loss constrained our ability to adjust these logits as desired. We sought for developing alternative measures for assessing the discrepancies between predicted and target probability distributions. This led us to a novel divergence function provided in Eqn. (4).

$$D(p, q) = e^p \cdot (p - q) \tag{4}$$

Here, p and q are predicted and target probability distributions, respectively. This simple divergence measure is tailored to highlight significant differences where the model has greater confidence in its predictions. The inclusion of the exponential term, e^p , scales the impact of these differences based on the size of p , thus providing a more sensitive measure in high-confidence regions. This aspect is particularly valuable in applications where the accuracy of high-confidence predictions is crucial. KL-divergence, with its logarithmic nature, tends to offer more stability during training, as it dampens the impact of large differences between p and q . This can be beneficial in preventing overfitting and ensuring a more gradual and stable learning process. However, the proposed divergence function is more responsive to high-confidence predictions due to its exponential term. This means it will aggressively adjust predictions where the model is very confident, potentially leading to faster convergence in those areas. In this domain, this property was helpful for adjusting peaks as we desired, by keeping the original low-value distributions in place (please refer to Section 4.3 for more discussions). Moreover, the function $e^p \cdot (p - q)$ demonstrates robustness in handling the numerical issues often encountered with small probabilities in traditional divergence calculations. By exponentially amplifying the divergence, it reduces the influence of minuscule probabilities, which are a common source of computational challenges in the KL divergence.

Utilizing this divergence function in our experimental work yielded encouraging outcomes, aligning effectively with our intuitive understanding of discrepancies in this domain. It provides an insightful and interpretable measure, especially in cases where conventional metrics do not fully capture the dynamics of model predictions. A comprehensive analysis of the proposed divergence function exceeds the scope of the current study and will be the subject of an upcoming follow-up paper.

3 Experimental Settings

We conducted our experiments using two prominent datasets in this field: CIFAR-10 and CIFAR-100. For the CIFAR-10 dataset, we employed a ResNet-18 model as the teacher network. A diverse range of student network architectures was tested, including a basic 5-layer CNN, ResNet-18 and two simplified ResNet architectures specifically tailored for CIFAR-10; ResNetC-20, ResNetC-32 by He et al. [23]. In experiments with the CIFAR-100 dataset, we explored the effects of network capacity and dataset complexity using ResNet-18 and ResNet-50 as teacher networks. For student networks in these experiments, we utilized ShuffleNetV2 [24], ResNet-18 and the respective teacher network architectures themselves. Our experimental setup, including configurations and parameters, closely followed those outlined in the *Nasty Teacher* study for a comprehensive comparison [17]. Specifically, the distillation temperatures (denoted as τ) for CIFAR-10 and CIFAR-100 were set at 4 and 20, respectively, in accordance with the recommendations from [17]. The weighting factor α was selected as 0.004 for

Table 1: Model accuracies obtained using CIFAR-10 dataset. In the Teacher Type column, the following abbreviations are used: ST for *Stingy Teacher*, BASE for Baseline Teacher, NT for *Nasty Teacher*, STT for Stingy Trained Teacher, and AST, our proposed model.

Model	Teacher Type	Teacher Acc.%	Student Accuracy			
			CNN	ResNetC20	ResNetC32	ResNet18
SBase	–	–	86.64	92.37	93.41	95.03
Res18	ST	95.03	83.11(-3.53)	67.98(-24.39)	74.08(-19.33)	92.47(-2.69)
Res18	BASE	95.03	87.76(+1.12)	92.27(-0.1)	92.94(-0.47)	95.39(+0.23)
Res18	NT	94.37(-0.67)	82.98(-6.62)	88.54(-3.73)	90.07(-2.87)	93.76(-1.63)
Res18	STT	94.94(-0.09)	86.70(+0.06)	91.30(-1.07)	91.85(-1.56)	94.48(-0.68)
Res18	ASD	94.61 (-0.42)	79.82 (-7.94)	87.08 (-5.19)	88.70 (-4.24)	93.66 (-1.73)

CIFAR-10 and 0.005 for CIFAR-100. Training of the basic CNN was carried out over 100 epochs with a learning rate of 0.001, using the Adam optimizer [25]. Other network architectures were trained using the SGD optimizer, incorporating a momentum of 0.9 and a weight decay of 0.0005. These networks are trained with an initial learning rate of 0.1, adjusting for CIFAR-10 over 160 epochs with reductions in the learning rate by a factor of 10 at the 80th and 120th epochs. For CIFAR-100, the training spanned 200 epochs, with learning rate adjustments by a factor of 5 at the 60th, 120th, and 160th epochs, adhering strictly to the protocol established in the *Nasty Teacher* publication [17].

In our distillation process, we closely follow the *Stingy Teacher* model, which shares the same settings as in the *Nasty Teacher*, with specific adjustments made to accommodate the model’s unique features. In this context, the sparsity ratios for these models are defined as 0.1 for CIFAR-10 and 0.2 for CIFAR-100, following the guidelines provided in the corresponding paper [19].

The training procedure for our models involves distinct configurations based on the dataset and model architecture. For the ResNet-18 *AST* model trained on the CIFAR-10 dataset, the setup includes a temperature parameter (τ) of 6, an α parameter of 0.05, and a sparsity ratio for logits of 0.2. When adapting this ResNet-18 *AST* model for the CIFAR-100 dataset, adjustments are made with the temperature parameter increased to 30, the α parameter set to 0.035, and the sparsity ratio of logits fine-tuned to 0.07. Furthermore, the training of the ResNet-50 *AST* model on the CIFAR-100 dataset maintains a temperature parameter of 30, but the α parameter is slightly reduced to 0.03, and the sparsity ratio of logits is kept at 0.07.

Projected Gradient Descent (PGD) attack [20], is implemented on images with the configuration settings as follows: the ϵ parameter, defining the maximum perturbation size, is established at 0.3; the step size for each iteration is determined to be 0.01; and the total number of iterative steps is fixed at 40.

In our experiments, we aimed to compare the *AST* approach with the *Stingy Teacher* method. However, it’s important to note that the original study on *Stingy Teacher* [19] did not involve training a teacher model. Instead, it creates an undistillable teacher by manually manipulating its outputs. In contrast, both our method and the *Nasty Teacher* [17] approach prioritize maintaining the accuracy of the teacher model while modifying its outputs in training stage, and these teachers works in a fully *white-box* setting. To facilitate a fair comparison between the *AST* and the *Stingy Teacher*, as well as to examine the impact of adversarial examples, we developed a trained teacher version of the *Stingy Teacher* model by replacing the outputs generated from adversarial examples with those from a baseline teacher model and then make these outputs sparse. All the other parameters remained consistent with those used in our *AST* model, including the loss function (i.e. EPD loss).

Table 2: Model accuracies obtained using CIFAR-100 dataset. In the Teacher Type column, the following abbreviations are used: ST for *Stingy Teacher*, BASE for Baseline Teacher, NT for *Nasty Teacher*, STT for *Stingy Trained Teacher*, and AST, our proposed model, for *AST*.

Model	Teacher Type	Teacher acc.%	Student Accuracy		
			ShuffleNetV2	ResNet18	Teacher
Std.	–	–	72.10	78.28	–
Res18	ST	78.28	50.49(-21.61)	55.30(-22.98)	55.30(-22.98)
Res50	ST	77.55	46.46(-25.64)	54.22(-24.06)	54.14(-23.41)
Res18	BASE	78.28	74.38(+2.28)	79.12(0.84)	79.12(0.84)
Res18	NT	77.80(-0.48)	65.01(-7.09)	74.68(-3.60)	74.68(-3.60)
Res18	STT	77.92 (-0.36)	68.47(-3.63)	77.42(-0.86)	77.42(-0.86)
Res18	AST	76.61(-1.67)	43.25 (-28.85)	65.90 (-12.38)	65.90 (-12.38)
Res50	BASE	77.55	74.00(+1.90)	79.27(+0.99)	80.03(+2.48)
Res50	NT	76.88(-0.67)	67.14(-4.96)	73.87(-4.41)	75.99(-1.56)
Res50	STT	77.25(-0.3)	70.28(-1.82)	76.16(-2.12)	77.50(-0.05)
Res50	AST	77.85 (+0.3)	43.18 (-28.92)	65.05 (-13.23)	62.81 (-14.74)

4 Results and Discussions

4.1 CIFAR-10 Experiments

Experimental results on CIFAR-10 are presented in Table 1. The SBase row is used for depicting the baseline performances of the student networks. In the Teacher accuracy column we want to obtain accuracy as close to Base model as possible. The experiments with CIFAR10 shows that AST (teacher) model performance is comparable with the other teacher models. In this context all three models BT, STT and ASD is performing similarly. However, we observe better performance (considerably lower scores) on the students that are distilled from AST. The Table shows the relative reductions in the student performances next to each score in parenthesis. ResNetC-20 and ResNetC-32 students show a minor accuracy drop of approximately 0.1% and 0.47% post KD from their baseline teacher performances, respectively. Other student architectures report improvements up to around 1%. In the comparison of KD effectiveness among NT and AST, which are similar methods that trains an undistillable teacher model to prevent knowledge transfer, both NT and AST lead to reduced student performance, particularly in simpler networks. However, AST surpasses NT in all students. Trained teacher version of ST, denoted as STT, showed slightly better teacher performance than AST but it remained insufficient in the context of defense against knowledge distillation.

Note that, *Stingy Teacher*(ST) model employs a different methodology, where only a subset of baseline teacher’s logits is revealed to the students without explicitly training a teacher model. This approach significantly impacts smaller ResNet models, surpassing AST’s performance. Nonetheless, for basic CNN student, to our surprise, AST could also outperform ST.

4.2 CIFAR-100 Experiments

The experimental results on CIFAR-100 are provided in Table 2. In this setting we conducted experiments using two different teacher architectures, ResNet18 and ResNet50. Since there are more categories in this dataset, we want to observe the effect of capacity increase to the KD performances. The results show that with the ResNet-18 architecture, AST model exhibits slightly lower performance compared to the NT and STT models. Conversely, when employing the more complex ResNet-50 architecture, AST surpasses all teacher models, including the baseline teacher.

Our proposed model demonstrates that in a fully transparent (full white-box) setting, i.e. when we compare AST with the trained teacher models, AST exhibits a more pronounced accuracy decline. In other words, it outperforms both NT and STT methods, which are fully trained teacher models for IP

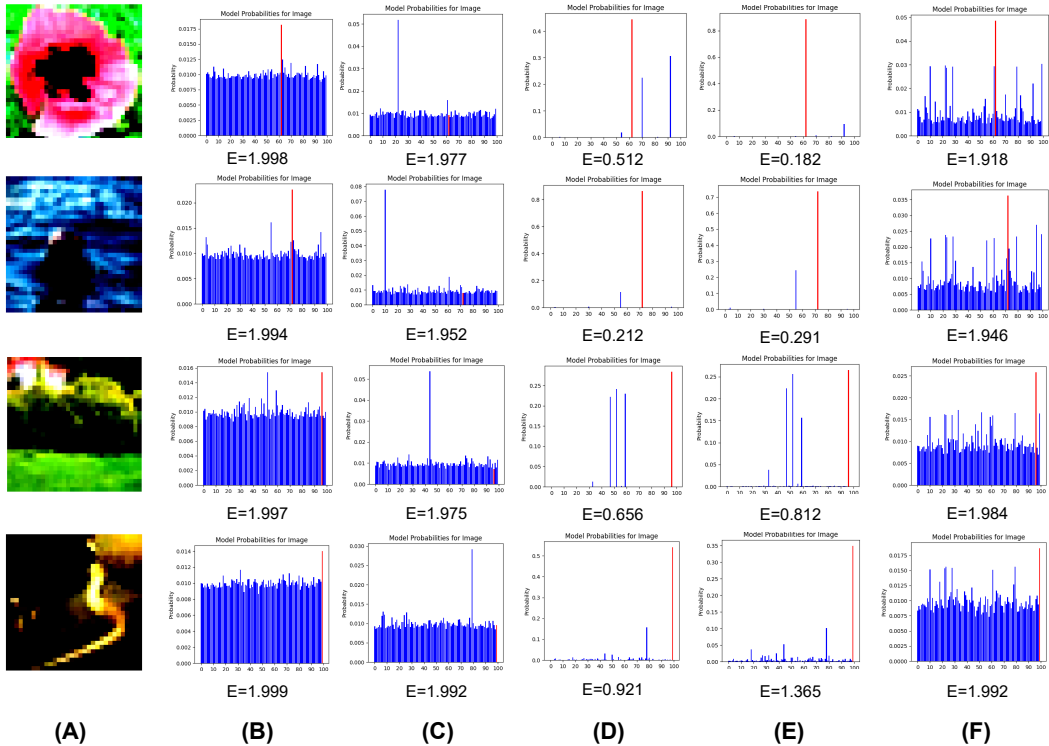


Fig. 2: Illustration of the logit responses after the application of softmax temperature. Columns depict the following information: (A) samples of clean images, (B) responses of the baseline model to these clean samples, (C) responses of the baseline model to the adversarial counterparts of the clean images, (D) responses of the NT model to clean samples, (E) responses of the STT model to clean images, (F) responses of our proposed method (AST) to clean images. Below each distribution, the entropy of the distributions are provided.

protection. Specifically, the performance of AST increases significantly for ShuffleNetV2 student models for both teacher architectures; around 28.9% decrease is observed in both ResNet18 and ResNet50 AST models compared to the baseline student model. The performance of AST in this student architecture is even better compared to corresponding ST models. Given that the only modification made during the creation of STT was altering the input to the teacher model, it can be inferred that adversarial sparse inputs have a more significant impact than only sparse inputs in the process of developing an undistillable teacher.

4.3 Qualitative and Quantitative Analysis

This section complements the previous experiment results with additional qualitative and quantitative analysis. Given that the CIFAR-100 dataset contains ten times more categories than the CIFAR-10 dataset, our focus will be on demonstrating the ResNet-18 model’s responses specifically for CIFAR-100. Output responses of different networks focusing on the baseline teacher, NT, STT, and AST models, are illustrated in Fig. 2. Similar to the approach in [19], we applied a softmax temperature to the logit responses to enhance visualization in this paper. Additionally, we present the output responses of the baseline teacher model to corresponding adversarial images (shown in the third column), and the entropy values of each distribution are displayed beneath them. The baseline model typically yields a nearly uniform distribution across classes, with a single peak in a class, demonstrating high confidence for both clean and adversarial images; frequently produce peaks for the correct class in the clean images and an incorrect class in the adversarial images. The distribution for adversarial image responses exhibits lower entropy compared to that for clean images. Contrary to these distributions, the distribution from the AST model reveals additional, sparse peaks. We attribute these peaks to our sparse optimization scheme (with EPD loss function), which generally does not exceed the true category in magnitude. We believe that the increased relative entropy, coupled with the additional sparse peaks, renders the distillation process more challenging for the student models.

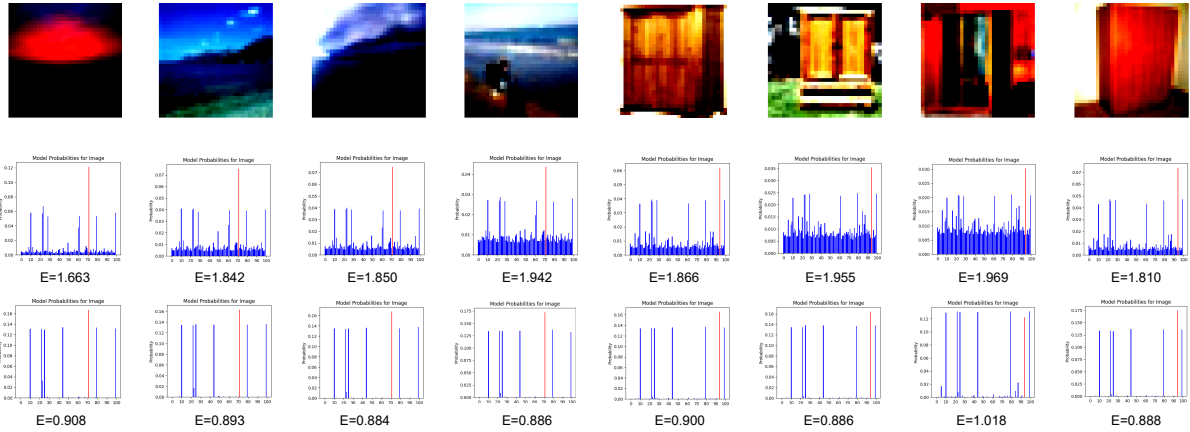


Fig. 3: The responses of our ResNet-18 AST model and AST trained with KL Divergence model to clean samples from two sets of identical classes is displayed. Top row: input images, middle-row: Responses of AST trained with EPD loss, last row: responses of AST trained with KL Divergence loss. Samples in the leftmost 4 columns and righthmost 4 columns belong to same classes. The softmax temperature applied to all logits and below each distribution, the entropy value is displayed.

Table 3: Within Class KL Divergences and Entropies of ResNet18 Model Outputs in CIFAR-100 for two categories.

Model	Label	KL Divergence				Entropy			
		Mean	Variance	Min	Max	Mean	Variance	Min	Max
BASE	0	0.00082	8.56e-8	0	0.00215	1.99831	4.63e-8	1.99626	1.99958
NT	0	0.49432	0.26566	0	3.63332	0.25185	0.14789	0.00895	1.68001
STT	0	0.20675	0.09579	0	2.3795	0.23811	0.09251	0.02666	1.58349
AST	0	0.02912	0.00072	0	0.12058	1.77491	0.01709	1.45852	1.99016
BASE	10	0.00161	2.61e-07	0	0.00286	1.99841	8.11e-7	1.99361	1.99954
NT	10	1.06778	1.20049	0	4.21843	0.70504	0.21716	0.00968	1.74953
STT	10	0.96356	0.73454	0	4.06417	0.67207	0.24490	0.06806	1.81497
AST	10	0.68240	0.33229	0	1.48405	1.55906	0.19533	0.84747	1.99639

In addition, we want to compare the ASL responses trained with EPD loss and KL-div loss within a specific class to examine our model’s general characteristics. In this context, Fig. 3 presents the models’ responses for randomly selected samples within the same category for two different categories. As observed in the figure, ASD (with EPD) model’s response characteristics are notably similar, characterized by high entropy (a uniform-like distribution across all categories), yet with sparse and relatively consistent peaks for a few classes (approximately 6-8). Notably, a higher peak is evident in the true category, which is highlighted in red. ASD (with KL-div) responses are more sparse. After the optimization, too much increase in the magnitude of sparse peaks inversely affects (degrades) the teacher performance. An illustrative example of this scenario can be observed in the seventh column of Fig. 3.

Furthermore, in order to quantify the characteristics of the model responses, we computed the entropies of the output distributions for the entire test set for all teacher models. The statistics of the entropy values are provided for two categories in Table 3. The quantitative results are on par with the qualitative results and consistent in different categories, where base teacher and AST output entropies are higher compared to NT and STT models. However, AST entropy variance is higher than the base teacher model, due to relatively peaky nature of the output distributions arising due to the sparseness constraint applied during training.

We further investigated the consistency of output distributions within the same classes by designing another set of measurements that involves randomly selecting a reference sample from two categories and calculating its relative entropy against the outputs of other samples in the same category. The findings, detailed in Table 3, indicate significant variability among the models. The base model consistently shows the lowest mean KL divergence for both labels, as expected, which suggests a closer correlation with

Table 4: The table presents the impact of different values of α and τ parameter on a ResNet-18 *AST* model trained using the CIFAR-100 dataset.

Acc%	α			τ		
	0.03	0.035	0.04	20	30	40
Teacher	76.27	76.61	76.16	76.94	76.61	75.54
Student	65.42	65.90	70.41	70.01	65.90	71.82

Table 5: The table represents the influence of different values of sparsity ratio on a ResNet-18 *AST* model trained using the CIFAR-100 dataset.

SR	Teacher	Student
	Acc.%	Acc.%
0.05	76.27	63.30
0.07	76.61	65.90
0.1	76.46	66.77
1	77.87	79.69

the expected distribution, denoting confident and precise model predictions. This is a desired property for recognition, yet not desirable for protection. In contrast, the NT model exhibits greater variance in KL divergence, particularly for label 10, reflecting a wider deviation from the standard distribution and potentially indicating less consistent predictions designed to mislead the student model. The STT model presents similar characteristics to the NT model but with a marginally reduced maximum KL divergence, suggesting a slightly tighter distribution. In comparison, the AST model achieves a lower KL divergence relative to the NT and STT models, yet higher than the base model, underscoring the stability of its output signals. Moreover, it presents a significantly greater variance in divergence values compared to the base model. Based on the entropy and KL divergence values, we can conclude that the desired outputs are being generated for misleading the student models.

4.4 Ablation Studies

We conducted experiments on different parameter settings using the Resnet-18 model and the CIFAR-100 dataset. Table 4 shows the influence of α parameter on the performance of an *AST* and an identical student through Knowledge Distillation (KD). Except for α all parameters held constant. The optimal teacher performance and defense were observed when the α parameter was set to 0.035. We also conducted an ablation study on the effect of temperature parameter, τ (Table 4). Optimal results are achieved with τ set to 30. We observed that, a higher value of τ leads to a decrease in the teacher’s performance and defensiveness.

We made ablation on the sparse ratio parameter, and the results are presented in 5. Each teacher with low sparsity ratios achieved significant reduction on student’s performance. A lower sparse ratio value led to a significant reduction on student performance, but decreasing or increasing this value also resulted in diminished teacher performance, which is unfavorable. SR set to 1 corresponds to the scenario where there is no sparsity constraint applied; in this condition, AST was unable to degrade the performance of the student network. Based on these findings, for our AST model, the sparse ratio parameter is set to 0.7.

As the final ablation study, we compare AST model performances using KL-divergence loss and our

Table 6: The table represents the influence of log-space on a ResNet-18 *AST* model trained using the CIFAR-100 dataset.

Loss Function	Teacher	Student
	Acc.%	Acc.%
KL-Div Loss	66.5	60.1
EPD Loss	76.6	65.9

proposed EPD loss in Table 6. Using EPD loss gave better results in teacher performance, yet, KL-div loss provides better student performance. However, the reduction in the student performance effected teacher performance significantly. EPD loss provided more balanced performance, keeping teacher performance around 10% higher, while redusing the student accuracy to 65.9%. In this experiments, all the factors firing the training is kept the same, only the loss function is changed.

5 Conclusion

In this study, we introduce a new training method for teacher networks called *AST*, designed to safeguard against knowledge theft through Knowledge Distillation. We developed a specialized loss function that minimizes the difference in responses between adversarial examples and clean images. Consequently, the *AST*'s responses are deliberately misleading, consistently providing incorrect information to deter adversaries. Our extensive experiments across different teacher-student architectures and datasets demonstrate the effectiveness of our approach. In scenarios where adversaries have complete knowledge, including access to training data, *AST* significantly impairs their performance. This method is particularly effective in complex teacher architectures and datasets, outperforming other strategies in fully-disclosed model scenarios.

We also introduce a novel divergence loss function (EPD) utilized in *AST* training that has proven effective in our empirical results. However, future research is vital to refine this approach and explore its broader implications, particularly in terms of computational efficiency and adaptability to various model architectures.

References

- [1] G. E. Hinton, O. Vinyals, and J. Dean, "Distilling the knowledge in a neural network," in *NIPS*, 2015.
- [2] S. I. Mirzadeh, M. Farajtabar, A. Li, N. Levine, A. Matsukawa, and H. Ghasemzadeh, "Improved knowledge distillation via teacher assistant," in *Proceedings of the AAAI conference on artificial intelligence*, vol. 34, pp. 5191–5198, 2020.
- [3] A. Romero, N. Ballas, S. E. Kahou, A. Chassang, C. Gatta, and Y. Bengio, "Fitnets: Hints for thin deep nets," in *3rd International Conference on Learning Representations, ICLR 2015, San Diego, CA, USA, May 7-9, 2015, Conference Track Proceedings* (Y. Bengio and Y. LeCun, eds.), 2015.
- [4] H. Chen, Y. Wang, C. Xu, C. Xu, and D. Tao, "Learning student networks via feature embedding," *IEEE Trans. Neural Networks Learn. Syst.*, vol. 32, no. 1, pp. 25–35, 2021.
- [5] N. Komodakis and S. Zagoruyko, "Paying more attention to attention: improving the performance of convolutional neural networks via attention transfer," in *ICLR*, 2017.
- [6] W. Park, D. Kim, Y. Lu, and M. Cho, "Relational knowledge distillation," in *Proceedings of the IEEE/CVF conference on computer vision and pattern recognition*, pp. 3967–3976, 2019.
- [7] N. Passalis, M. Tzelepi, and A. Tefas, "Heterogeneous knowledge distillation using information flow modeling," in *Proceedings of the IEEE/CVF Conference on Computer Vision and Pattern Recognition*, pp. 2339–2348, 2020.
- [8] B. Peng, X. Jin, J. Liu, D. Li, Y. Wu, Y. Liu, S. Zhou, and Z. Zhang, "Correlation congruence for knowledge distillation," in *Proceedings of the IEEE/CVF International Conference on Computer Vision*, pp. 5007–5016, 2019.
- [9] J. Gou, B. Yu, S. J. Maybank, and D. Tao, "Knowledge distillation: A survey," *International Journal of Computer Vision*, vol. 129, pp. 1789–1819, 2021.
- [10] L. Zhang, J. Song, A. Gao, J. Chen, C. Bao, and K. Ma, "Be your own teacher: Improve the performance of convolutional neural networks via self distillation," in *2019 IEEE/CVF International Conference on Computer Vision (ICCV)*, pp. 3712–3721, 2019.
- [11] L. Yuan, F. E. Tay, G. Li, T. Wang, and J. Feng, "Revisiting knowledge distillation via label smoothing regularization," in *Proceedings of the IEEE/CVF Conference on Computer Vision and Pattern Recognition*, pp. 3903–3911, 2020.
- [12] M. Xue, Y. Zhang, J. Wang, and W. Liu, "Intellectual property protection for deep learning models: Taxonomy, methods, attacks, and evaluations," *IEEE Trans. Artif. Intell.*, vol. 3, no. 6, pp. 908–923, 2022.
- [13] Y. Adi, C. Baum, M. Cisse, B. Pinkas, and J. Keshet, "Turning your weakness into a strength: Watermarking deep neural networks by backdooring," in *27th USENIX Security Symposium (USENIX Security 18)*, pp. 1615–1631, 2018.
- [14] Y. Uchida, Y. Nagai, S. Sakazawa, and S. Satoh, "Embedding watermarks into deep neural networks," in *Proceedings of the 2017 ACM on international conference on multimedia retrieval*, pp. 269–277, 2017.

- [15] L. Fan, K. W. Ng, and C. S. Chan, “Rethinking deep neural network ownership verification: Embedding passports to defeat ambiguity attacks,” *Advances in neural information processing systems*, vol. 32, 2019.
- [16] J. Zhang, D. Chen, J. Liao, W. Zhang, G. Hua, and N. Yu, “Passport-aware normalization for deep model protection,” *Advances in Neural Information Processing Systems*, vol. 33, pp. 22619–22628, 2020.
- [17] H. Ma, T. Chen, T.-K. Hu, C. You, X. Xie, and Z. Wang, “Undistillable: Making a nasty teacher that cannot teach students,” in *ICLR*, 2021.
- [18] S. Kullback, *Information theory and statistics*. Courier Corporation, 1997.
- [19] H. Ma, Y. Huang, H. Tang, C. You, D. Kong, and X. Xie, “Sparse logits suffice to fail knowledge distillation,” in *ICLR*, 2022.
- [20] A. Madry, A. Makelov, L. Schmidt, D. Tsipras, and A. Vladu, “Towards deep learning models resistant to adversarial attacks,” in *ICLR*, 2018.
- [21] H. Kannan, A. Kurakin, and I. J. Goodfellow, “Adversarial logit pairing,” *CoRR*, vol. abs/1803.06373, 2018.
- [22] I. J. Goodfellow, J. Shlens, and C. Szegedy, “Explaining and harnessing adversarial examples,” in *ICLR*, 2015.
- [23] K. He, X. Zhang, S. Ren, and J. Sun, “Deep residual learning for image recognition,” in *Proceedings of the IEEE conference on computer vision and pattern recognition*, pp. 770–778, 2016.
- [24] N. Ma, X. Zhang, H.-T. Zheng, and J. Sun, “Shufflenet v2: Practical guidelines for efficient cnn architecture design,” in *Proceedings of the European conference on computer vision (ECCV)*, pp. 116–131, 2018.
- [25] D. P. Kingma and J. Ba, “Adam: A method for stochastic optimization,” *arXiv preprint arXiv:1412.6980*, 2014.